Institute of Paper Science and Technology

AIR/SHEET INTERACTIONS

Project 3730/F006

Report 1

to the

MEMBER COMPANIES OF THE INSTITUTE OF PAPER SCIENCE AND TECHNOLOGY

August 1994

IPST

Atlanta, Georgia

INSTITUTE OF PAPER SCIENCE AND TECHNOLOGY
PURPOSE AND MISSION STATEMENT

The Institute of Paper Science and Technology is a unique organization whose charitable, educational, and scientific purpose evolves from the singular relationship between the Institute and the pulp and paper industry which has existed since 1929. The purpose of the Institute is fulfilled through three missions, which are:

- to provide high quality students with a multidisciplinary graduate educational experience which is of the highest standard of excellence recognized by the national academic community and which enables them to perform to their maximum potential in a society with a technological base; and
- to sustain an international position of leadership in dynamic scientific research which is participated in by both students and faculty and which is focused on areas of significance to the pulp and paper industry; and
- to contribute to the economic and technical well-being of the nation through innovative educational, informational, and technical services.

ACCREDITATION

The Institute of Paper Science and Technology is accredited by the Commission on Colleges of the Southern Association of Colleges and Schools to award the Master of Science and Doctor of Philosophy degrees.

NOTICE AND DISCLAIMER

INSTITUTE OF PAPER SCIENCE AND TECHNOLOGY

Atlanta, Georgia

AIR/SHEET INTERACTIONS

Project 3730/F006

Report 1

A Progress Report

to the

MEMBER COMPANIES OF THE INSTITUTE OF PAPER SCIENCE AND TECHNOLOGY

By

C.K. Aidun

August 1994

TABLE OF CONTENTS

PROJECT 3730 -AIR/SHEET INTERACTIONS

Project Leader: Cyrus K. Aidun

PROGRAM OBJECTIVES

The objectives of this project are to: a) gain a better understanding of the fluid dynamics and the structural mechanics of sheet flutter; b) correlate the onset of break or sheet damage ("pain threshold") with the sheet flutter characteristics (e.g., frequency, speed, ...) and the sheet's structural properties; and c) extened of the results to analysis of blade deformation and vibration in coating processes.

The interactions between fluid flow and flexible solid boundaries will be examined with applications to processes in paper manufacturing. The primary application is in sheet vibration induced by interactions between the sheet and the adjacent air stream which results in operational difficulties and web breaks.

SUMMARY OF PROGRESS

This is the second year of this project, and many of the initial tasks involving development of the techniques required for computational and experimental studies of the air/sheet interactions have been completed.

We are developing a computational program to evaluate the three-dimensional surface deformation of the substrate under load and transform of coordinates from global to the local surface deformation system. The initial computational experiments demonstrated the potential of this approach in terms of air/sheet interactions, as well as optimization of moisture removal from the dryer section. Based on the initial two-dimensional, low-speed computations, the PAC members (Ben Thorp, Chairman) suggested that we file an invention disclosure form for a more effective ventilation in the dryer section. The Invention Disclosure is attached to this report.

The two-dimensional program for the solution of the full equations governing the fluid flow with rigid boundaries has been completed. Several sample problems have been solved to confirm the correctness and accuracy of the formulation and the solution methodology. The complete formulation for this part of the program is outlined below.

In the last report, we outlined the results from a series of wind tunnel experiments to evaluate the system for an in-depth study of sheet fluttering and mechanisms of reducing the vibration and consequent sheet breaks. Problems with these experiments were identified and resolved. The samples used in the wind-tunnel experiments were Bond #4 printing paper, Letter Print (IPST Letterhead) paper, unbleached paperboard (Corrugating Medium), and light-weighted "trace" paper. Once the computational methods are fully developed, the experimental data can be used to evaluate the solution.

BACKGROUND

The fluttering of a moving web is often analyzed by using the "threadline" model, one that assumes the entire width of the web deflects together, and neglects cross-directional variation of web motion. This model was studied by Pramila [1], who combined separate theories of the dynamics of axially moving material and hydrodynamics to include aerodynamic terms in the model By simply adding the mass of surrounding air to the mass of the web, an "added mass" model was obtained. Pramila also assumed that the web is in an infinite air space and all the surrounding air move at the same speed as the web. In later studies, it has been demonstrated that the interaction between web and surrounding air is an important contributor to web instability and should therefore be taken into account.

In a later article, Pramila [2] assumes the air to be stationary, moving only in planes perpendicular to the x-axis. This consideration was taken into account by summing the added mass to the first term of the equation of motion only, rather than to all inertia terms, as was done in Pramila [1]. Although analytical results showed that the rate of decrease of natural frequency fares slightly better on this assumption, no definite conclusion could be drawn.

The "threadline model" was used again by Chang and Moretti [3] to study the out-of-plane flutter of a moving web. They showed that each of the dynamic terms in the governing equation - namely the transverse acceleration, Coriolis, and centrifugal forces - are affected differently by the air, depending on the air flow and the surrounding enclosure. They also determined the influence of parallel air flow and detected two different instabilities - steady deflection and flutter.

In the article by Race et al. [4], an investigation into the air movement induced by felts and fabrics was undertaken. The object was to determine the cause of sheet flutters experienced in f

first dryer sections of newsprint-making machines, with special attention placed on the surface roughness and permeability of the felt or fabric. The study also tested the claim that, by using felts and fabrics of high permeability of the dryer sections of paper machines, an induced ventilation effect will be obtained, resulting in an increase of the drying rate. What the study found was that the volume of air "pumped" through a fabric is dependent only on the fabric permeability itself and not on the surface roughness as was presupposed. It also found that the ventilating effect resulting from the use of a fabric is governed not only by the felt permeability, but by the machine speed, too. These findings helped papermakers to eliminate the possibility of surface roughness as a contributor to the problems of sheet flutter and provide them with a better idea of where to use felt or fabric at different parts of the papermaking machine.

In studying the physics of paper machine sheet flutter, Soininen [5] suggested that air flows do not generally create the edge flutter as often assumed, but instead, the edge flutter produces such air flows that the transversal wave energy component is dissipated to the air. He, then, concluded that the main reason for sheet flutter is a variation of basis weight of the sheet.

The idea of visualizing air flows by colored smoke documented by Sieverding and Bosche [6] was also used in these preliminary experiments with a limited degree of success.

PHYSICALLY BASED COMPUTATIONAL ANALYSIS

Computational analysis based upon physical principles represents a promising technique in investigation of many papermaking processes. The dynamics of a deformable object in response to some applying force can be analyzed by including the relevant physical properties of the solid and the liquid phases. The deformable model is governed by the mechanical laws of continuous bodies whose shapes can change over time. These principles, expressed in the form of dynamic differential equations, unify the description of shape and motion. By solving the equations numerically, a realistic analysis of the problem involving the interaction of the deformable object with the surrounding fluid becomes possible. By varying input parameters, the dependency of the system's behavior on physical parameters or boundary conditions may be examined. The two cases that we shall consider are the elastohydrodynamics of blade coating and the air/sheet interactions in this project. The basic principles and approach in analyzing both cases are virtually the same.

In this project, however, we focus on air/sheet interactions. This problem consists of a deformable sheet under tension and exposed to varying air interactions. These variations include the sheet velocity and the air/sheet *angle of attack*. Taking the many possible complex configurations of wave patterns forming by the sheet, the case under investigation poses a very complex continuum mechanics problem. Therefore, it is appropriate to start with a rather simplified version of the problem and gradually introduce physical complications until the full complex and realistic system is considered. The overall approach can be summarized in the form of a block diagram presented below.

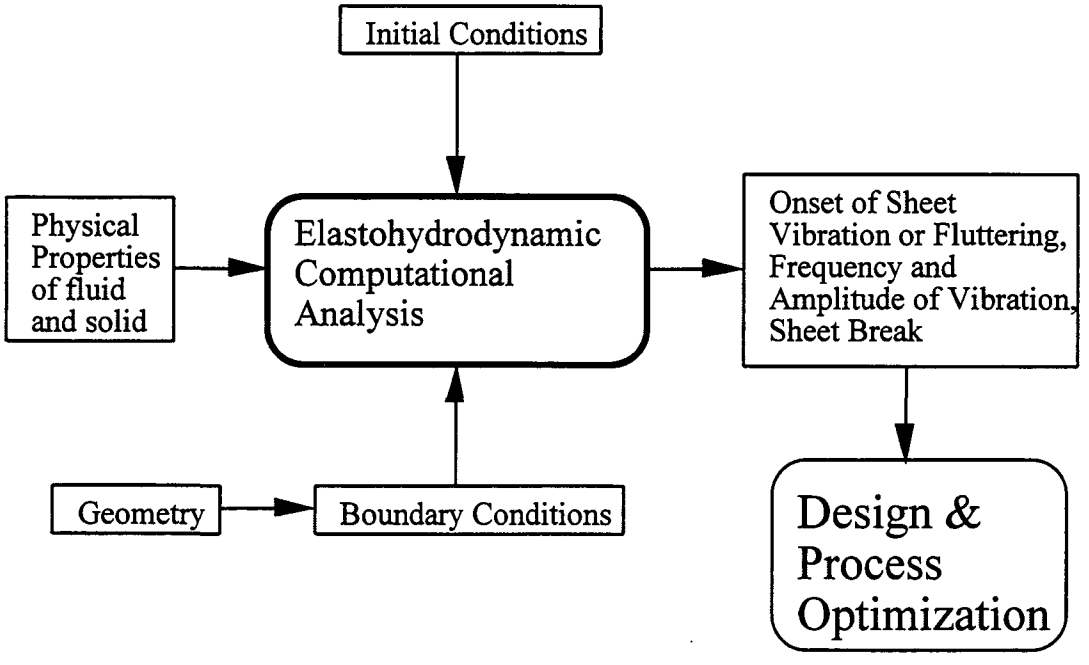

Figure 1. Block diagram of the computational approach.

The mathematical formulation for the coordinate deformation and mapping of the boundary to a local coordinate was presented in the last report. In this report, we outline the computational method for the more challenging part of the project, that is the fluid flow and interactions with the boundary.

The mathematical formulation and the solution procedure for the air flow with a rigid boundary are outlined below. The computational procedure, as outlined here, is formulated and implemented in general terms. Therefore, this method can be applied to any section of the paper machine. Tensor notation is used in explaining the dependence of the variables to the spatial coordinates. Accordingly, repeated indices imply

summation over the three spatial directions. An index following a comma indicates partial derivative of the variable with respect to the corresponding spatial coordinate. The variables are defined in the text following each equation.

The Navier-Stokes equations, which describe the flow of a steady, viscous, incompressible Newtonian fluid with constant properties, written in terms of primitive variables are

$$\rho u_\beta u_{\alpha,\beta} = \tau_{\alpha\beta,\beta} \tag{1}$$

and

$$u_{\beta,\beta} = 0 \tag{2}$$

where

$$\tau_{\alpha,\beta} = -p\delta_{\alpha\beta} + \mu(u_{\alpha,\beta} + u_{\beta,\alpha}) \tag{3}$$

x_α is the position in Cartesian coordinates; u_α is the velocity component in α −direction, p is the pressure derivation from hydrostatic; ρ is the fluid density; μ is the fluid viscosity; and $\delta_{\alpha\beta}$ is the Kronecker delta.

On each segment of the boundary, $\partial\Omega$, of the computational domain, Ω, it is necessary to prescribe appropriate boundary conditions. A precise statement of mathematically legitimate boundary conditions (in the sense of well posedness) for the Navier-Stokes equations often does not exist. A couple examples are open, or outflow, boundary conditions and free/moving boundary conditions (Gresho 1992; Christoudoulou and Scriven 1989; Sackinger et al. 1989; Kistler and Scriven 1984). Hence, there is understandable ambiguity, and even confusion, when boundary conditions are selected for numerical simulations. The boundary conditions relating to the momentum equations commonly employed are either the specification of the velocity components

$$u_\alpha = \tilde{u}_\alpha(s) \tag{4}$$

or specification of the surface stresses

$$n_\beta \tau_{\alpha\beta} = \tilde{\tau}_\alpha \tag{5}$$

where s is a parameter measuring position along the relevant boundary segment, and $\underline{n}(s)$ is the outward normal to the boundary.

Finite-Element Formulation

Only for limited cases do analytic solutions of the Navier-Stokes equations exist. For most problems of engineering interest, the Navier-Stokes equations are solved numerically. Difficulties in obtaining the numerical solution are related to the following: (1) the irregular geometries of the considered domain; (2) the equations are strongly coupled; (3) the equations are inherently nonlinear in the convection terms; (4) for convection-dominated flows, i.e. Re >> O(1), if the employed grid resolution is not fine enough, non-physical oscillations are prone to occur (Gresho and Lee 1981); (5) the continuity equation which regulates the pressure solution does not explicitly include the pressure variable (Sani et al. 1981a, b; Patankar 1980).

There are other versions of the Navier-Stokes equations derived from the "primitive" equations, such as the pressure Poisson equation and vorticity transport equation. Gresho (1991) has shown that the use of a primitive-variable form has some distinct advantages. In the following, the formal derivation of the Galerkin equations of the Navier-Stokes equations based on the primitive variables is presented (Gunzburg 1989; Curvelier 1986; Thomasset 1981).

Weak Form

The finite-element spatial discretization is performed using the Galerkin method. Within each element, the velocity and pressure fields are approximated by piecewise polynomial basis sets

$$u_\alpha^h(x_\beta) = \phi^T(x_\beta)U_\alpha \tag{6}$$

$$p^h(x_\beta) = \varphi^T(x_\beta)P \tag{7}$$

where U_α and P are column vectors of element nodal point, $\phi(x_\beta)$ and $\varphi(x_\beta)$ are column vectors of the interpolation functions, and the superscript T represents the transpose. Herein the same basis functions are employed for all components of the velocity.

Substitution of these approximations into the governing equations and the boundary conditions yields a set of equations:

$$\text{Momentum: } f_1(\phi,\varphi,U_i,P) = R_1 \tag{8}$$
$$\text{Continuity: } f_2(\varphi,U_i) = R_2 \tag{9}$$

where R_1 and R_2 are the residuals (errors) resulting from the use of the approximations (6) and (7).

The Galerkin form of the Method of Weighted Residuals seeks to reduce these errors to zero, in a weighted sense, by making the residuals orthogonal to the test functions of each element (i.e., ϕ *and* φ). These orthogonality conditions are expressed by

$$\text{Momentum: } (f_1,\phi) = (R_1,\phi) = 0 \tag{10}$$
$$\text{Continuity: } (f_2,\varphi) = (R_2,\varphi) = 0 \tag{11}$$

where (a,b) denotes the inner product, defined as

$$(a,b) = \int_\Omega a \cdot b \, d\Omega \tag{12}$$

A detailed derivation of the weak form of the Navier-Stokes equations, (1) - (3), and associated boundary conditions, (4) and (5), is given in Appendix A. The final forms are

$$\left(U_\beta^k \int_\Omega \rho\phi_i\phi_k\phi_{j,\beta}\right)U_\alpha^j + \left(\int_\Omega \mu\phi_{i,\beta}\phi_{j,\beta}\right)U_\alpha^j - \left(\int_\Omega \phi_{i,\alpha}\varphi_j\right)P_j = \int_{\partial\Omega} \phi_i \tilde{\tau}_\alpha \text{ ; i = 1, 2, ..., L} \tag{13}$$

$$\left(\int_\Omega \varphi_j\phi_{i,\alpha}\right)U_\alpha^i = \underline{0} \text{ ; j = 1, 2, ..., M} \tag{14}$$

where L and M are the number of velocity and pressure nodes, respectively, in the discrete domain.

Matrix Form

The component equations (13) and (14) can be combined into a single matrix equation

$$\text{Momentum}: \quad [\underline{\underline{N}}(\underline{U}) + \underline{\underline{K}}]\underline{U} + \underline{\underline{C}}\underline{P} = \underline{f} \tag{15}$$

and

$$\text{Continuity}: \quad \underline{\underline{C}}^T \underline{U} = \underline{0} \tag{16}$$

or in a more general format as

$$\underline{\underline{A}}(\underline{w})\underline{w} = \underline{b}(\underline{w}) \tag{17}$$

where

$$\underline{w}^T = \{\underline{U}^T, P^T\} \tag{18}$$

The definitions of the matrices $\underline{\underline{N}}(\underline{U})$, $\underline{\underline{K}}$, $\underline{\underline{C}}$, and $\underline{f}$ are given in Appendix A.

Pressure Modes and Requirement for Mixed Interpolation

The process of "element selection" and "underlying finite-dimensional approximation space" for both velocity and pressure is presented in this section. Early published finite-element solutions of the Navier-Stokes equations employed a so called "equal interpolation"; i.e. $\varphi = \phi$ (Hood and Taylor 1973). The authors noticed that an accurate solution for the velocity was usually accompanied by a very poor (or meaningless) pressure solution. When "mixed interpolation" (or "unequal interpolation") was employed, in which φ is one order lower (in polynomial degree) than ϕ, both velocity and pressure results appeared to be more reasonable (Hood and Taylor 1974).

Sani et al. (1981a, b) and Olson and Tuann (1978) made significant progress toward providing an explanation for the occurrence of the spurious pressure solutions. They concluded that equal interpolation generally results in a singular matrix with associated zero eigenvalues. These spurious pressure solutions (pressure modes) are simply an artifact of the discretization method employed - "basis functions" in finite element method (FEM) and "grid selection and variable locations" in finite difference method (FDM) of the Navier-Stokes equations, which also display spurious pressure modes (Patankar 1980).

The significant difficulties associated with the singular limit can be easily appreciated and the spurious pressure mode better understood by considering the following simple example with only two equations:

$$\begin{bmatrix} 1 & 0 \\ 0 & 0 \end{bmatrix} \begin{Bmatrix} \lambda_1 \\ \lambda_2 \end{Bmatrix} = \begin{Bmatrix} 1 \\ 0 \end{Bmatrix} \tag{19}$$

The matrix has eigenvalues $\lambda_1 = 1$, $\lambda_2 = 0$ and the linear system has the solution $\{1\ ,\ \ c\}^T$, where c is arbitrary. A small perturbation in the off-diagonal elements gives

$$\begin{bmatrix} 1 & \varepsilon \\ \varepsilon & 0 \end{bmatrix} \begin{Bmatrix} \hat{\lambda}_1 \\ \hat{\lambda}_2 \end{Bmatrix} = \begin{Bmatrix} 1 \\ 0 \end{Bmatrix} \tag{20}$$

The matrix now has eigenvalues $\hat{\lambda}_1 = (1+\sqrt{1+4\varepsilon^2})/2 \cong 1+\varepsilon^2$ and $\hat{\lambda}_2 = (1-\sqrt{1+4\varepsilon^2})/2 \cong -\varepsilon^2$, and the algebraic system has the solution $\{0,\ \ \varepsilon^{-1}\}^T$. The first component is changed by O(1) and the second by O(ε^{-1}); furthermore, the unperturbed solution cannot be recovered by letting ε approach zero. Fortunately, the useful pressure information can be recovered from the spurious pressure solution using smoothing techniques (Hughes et al. 1979, Lee et al. 1979, Hinton and Campbell 1974).

Because of the choice of pressure discretization, the resulting discrete system of equations may involve ill-conditioning and round-off error in practice. Pelletier et al. (1989) have invented several inexpensive techniques to minimize the effect of round-off error based on the measurement of incompressibility for the discrete divergence of the velocity field and recommended the use of discontinuous, C^{-1}, pressure approximations, particularly for strongly coupled flow problems. The element employing discontinuous (C^{-1}) can guarantee element level mass balances, $\int_{\Omega^e} \nabla \cdot \underline{u}^h = 0$, which must be judged as an additional advantage. Continuous (C^0) pressure approximation, on the other hand, can only be shown to yield a global mass balance (Gresho et al. 1980). Bercovier and Engelman (1979) have also demonstrated the superiority of the nine-node isoparametric quadrilateral element over the eight-node (serendipity) element in many computational experiments. Therefore we use 9-node Lagrange element for velocity interpolation and 4-node discontinuous bilinear interpolation for the pressure in our study. The pressure degrees of freedom are located at the four points of 2×2 Gaussian integration points.

Solution Procedure

The discrete system resulting from a finite-element discretization of the Navier-Stokes equations consists of a nonlinear system of algebraic equations. In order to improve the performance of the solution algorithms, all equations in the problem are solved in a fully coupled manner. Both the solution method for a system of equations and the solution

algorithm for the nonlinear system of equations are major factors influencing the efficiency of the finite-element program.

The major computational effort in any finite element procedure is expended in the solution of the assembled matrix equations that describe the discretized problem. The solver adopted to determine this solution has a significant bearing on the computer storage requirements and execution time. Of the many techniques available, the direct elimination frontal equation solution technique originated by Iron (1970) has earned the reputation of being easy and inexpensive to use. The main idea of the frontal solver is to assemble the equations and eliminate the variables at the same time. As soon as the coefficients of an equation are completely assembled from the contribution of all relevant elements, the corresponding variable can be eliminated. Therefore, the complete global matrix is never actually formed, since all reduced equations can be eliminated from core storage and stored on disc. Following the completion of equation assembly and reduction element-by-element, the stored information is used during the back substitution process to obtain the solution.

For highly coupled, nonlinear equations such as the Navier-Stokes equations, questions arise regarding the ability of the numerical algorithm to achieve a solution in addition to the computational efficiency. The choice of a solution algorithm is therefore a critical element in the overall utility, robustness and efficiency of a computer code. The most common methods employed, (a) successive-substitution method and (b) Newton's method, are summarized as follow:

(a) Successive-Substitution Method

A particularly simple iterative method with a large radius of convergence is the successive substitution (Picard, functional iteration) method. Application of the method for (17) is described by

$$\underline{\underline{A}}(\underline{w}^n)\underline{w}^{n+1} = \underline{b}(\underline{w}^n) \tag{21}$$

where the superscripts indicate the iteration levels. For strongly nonlinear problems the rate of convergence of (21) is fairly slow since it is a first-order method. An improvement in the convergence rate can sometimes be realized by use of a relaxation formula where

$$\underline{\underline{A}}(\underline{w}^n)\underline{w}^* = \underline{b}(\underline{w}^n) \tag{22}$$

and

$$\underline{w}^{n+1} = \alpha\underline{w}^n + (1-\alpha)\underline{w}^*, \quad 0 \le \alpha \le 1 \tag{23}$$

where α is the relaxation factor.

(b) Newton Method

In order to improve significantly on the rate of convergence, a second-order method, such as Newton's method, can be considered. Rewriting (17) as

$$\underline{R}(\underline{w}) = \underline{\underline{A}}(\underline{w})\underline{w} - \underline{b}(\underline{w}) \tag{24}$$

Then Newton's method can be expressed as

$$\underline{R}(\underline{w}^n) = -\frac{\partial \underline{R}}{\partial \underline{w}}\Big|_{\underline{w}^n} (\underline{w}^{n+1} - \underline{w}^n) = -\underline{\underline{J}}(\underline{w}^n)(\underline{w}^{n+1} - \underline{w}^n) \tag{25}$$

which can be solved for $\underline{w}^{n+1}$ as

$$\underline{w}^{n+1} = \underline{w}^n - \underline{\underline{J}}^{-1}(\underline{w}^n)\underline{R}(\underline{w}^n) \tag{26}$$

where $\underline{\underline{J}}(\underline{x})$ is the Jacobian matrix. The Newton scheme has a superior rate of convergence compared to the simple algorithm in (21). However, Newton's method also has a somewhat smaller radius of convergence (i.e., is more sensitive to the initial guess of $\underline{w}^0$). The Newton method can at times be improved by the use of a relaxation procedure similar to the one shown in (22) and (23). In some cases a sequential application of (21) and (26) provides the best method of solution.

Application to a Closed Dryer Section

The numerical method outlined above is being developed for analysis of air/sheet interactions in the paper machine. We have had good progress in the computational front. We can now solve for the air stream in very complex geometries as shown in Fig. 2 where the air stream in a closed dryer section of the paper machine has been simulated. The figure shows the air particle trajectories in the dryer section. As shown here, recirculating eddies form and trap the moisture near the rolls. At the left section, air is dragged with the felt and the paper into the lower nip encountering a high pressure region, it returns in a jetting action to impinge on the surface of the top roll. A similar pattern forms between the paper and the roll in the other section.

When these initial results were presented at the Project Advisory Committee meeting, our PAC chairman suggested that we can use these results to better ventilate and remove moisture from the dryer section. We now have an invention disclosure for a more efficient moisture removal mechanism (see appendix B).

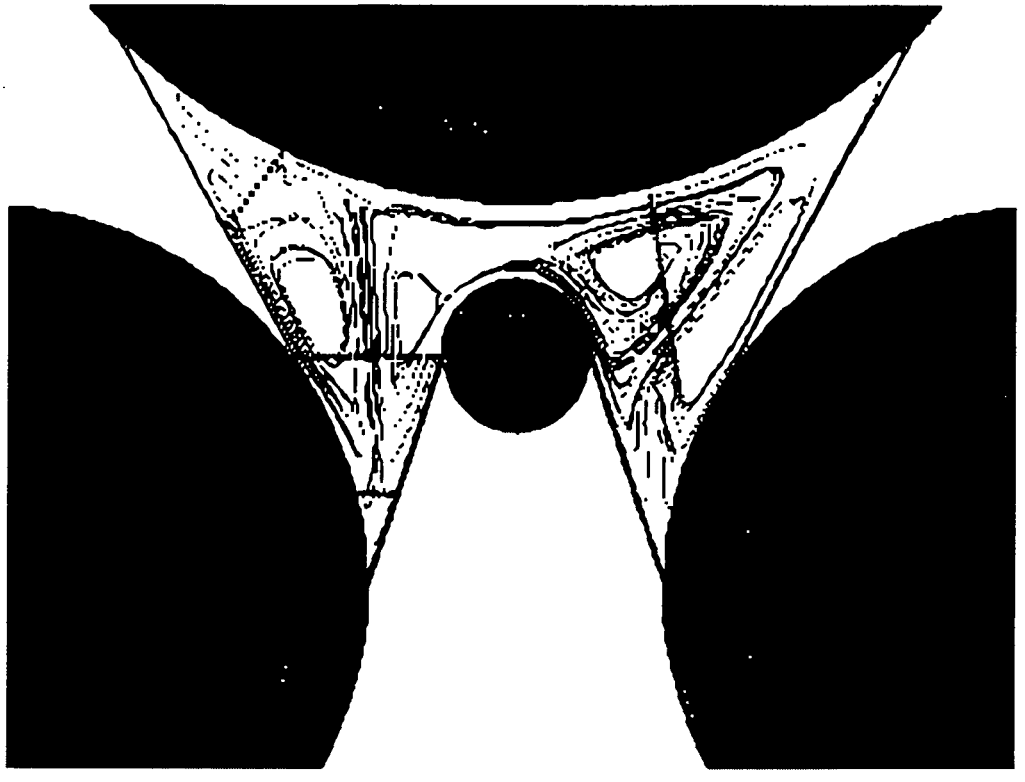

Figure 2. Air stream in a closed section of the dryer showing the formation of recirculating eddies and jet impingement on the surface of the roll at the left section and the felt on the right section. The two converging nips are singular points of high pressure. The dots show the location where the particles are released for visualization purposes.

Appendix A

The weak form of momentum equation, (1), and associated boundary conditions, (4) and (5), is obtained by first multiplying the equation by any of the velocity basis function (i.e., by a test function), ϕ_i , i = 1, 2, ..., L where there are L velocity nodes in the discretized domain, and integrating over the domain, Ω.

$$\int_{\Omega} \phi_i \rho u_\beta u_{\alpha,\beta} = \int_{\Omega} \phi_i \tau_{\alpha\beta,\beta} \tag{A-1}$$

Then, since $\phi_i \tau_{\alpha\beta,\beta} = \left(\phi_i \tau_{\alpha\beta}\right)_{,\beta} - \phi_{i,\beta}\tau_{\alpha\beta}$, and from the divergence theorem

$$\int_{\Omega} \left(\phi_i \tau_{\alpha\beta}\right)_{,\beta} = \int_{\partial\Omega} \phi_i n_\beta \tau_{\alpha\beta} \tag{A-2}$$

where $\partial\Omega$ is the boundary of Ω and n_α is the α −component of the outward unit normal vector on $\partial\Omega$. To incorporate the boundary condition, (5), $n_\beta \tau_{\alpha\beta} = \tilde{\tau}_\alpha$, (A-1) becomes

$$\int_{\Omega} \phi_i \rho u_\beta u_{\alpha,\beta} = \int_{\partial\Omega} \phi_i n_\beta \tau_{\alpha\beta} - \int_{\Omega} \phi_{i,\beta}\tau_{\alpha\beta} = \int_{\partial\Omega} \phi_i \tilde{\tau}_\alpha - \int_{\Omega} \phi_{i,\beta}\tau_{\alpha\beta} \tag{A-3}$$

Similarly, the appropriate weak form of continuity equation, (2), is obtained by multiplying it by any one of the pressure basis functions (as a test function), say φ_j , j = 1, 2, ..., M where there are M pressure "nodes" - they are located at the 2×2 Gaussian integration points in each element - in the discretized domain. Thus (2) becomes, in the weak form

$$\int_{\Omega} \varphi_j u_{\alpha,\alpha} = 0 \;\; ; \;\; j = 1,2,\ldots,M \tag{A-4}$$

Using the definition of the Galerkin procedure, (8) and (9), and the finite element approximations, (6) and (7), (A-3) and (A-4) can be written as

$$\left(U_\beta^k \int_{\Omega} \rho \phi_i \phi_k \phi_{j,\beta}\right) U_\alpha^j + \left(\int_{\Omega} \mu \phi_{i,\beta} \phi_{j,\beta}\right) U_\alpha^j - \left(\int_{\Omega} \phi_{i,\alpha} \varphi_j\right) P_j = \int_{\partial\Omega} \phi_i \tilde{\tau}_\alpha \; ; \; i = 1, 2, \ldots, L \tag{A-5}$$

and
$$\left(\int_{\Omega} \varphi_j \phi_{i,\alpha}\right) U_\alpha^i = \underline{0} \ ; \ j = 1, 2, ..., M \tag{A-6}$$

The corresponding matrix equations (ODE's) can be written in the condensed form

$$[\underline{\underline{N}}(\underline{U}) + \underline{\underline{K}}]\underline{U} + \underline{\underline{C}}\underline{P} = \underline{f} \tag{A-7}$$
$$\underline{\underline{C}}^T \underline{U} = \underline{0} \tag{A-8}$$

Where now $\underline{U}$ is a global vector of length d*L, where d is the number of dimensions, and $\underline{P}$ is a global M-vector of pressures. The associated matrices for the two-dimensional situation can be explicitly expressed as

$$\underline{\underline{N}}(\underline{U}) = \begin{bmatrix} U_k \int_{\Omega} \rho \phi_i \phi_k \phi_{j,x} + V_k \int \rho \phi_i \phi_k \phi_{j,y} & \underline{0} \\ \underline{0} & U_k \int_{\Omega} \rho \phi_i \phi_k \phi_{j,x} + V_k \int_{\Omega} \rho \phi_i \phi_k \phi_{j,y} \end{bmatrix} \tag{A-9}$$

$$\underline{\underline{K}} = \begin{bmatrix} \int_{\Omega} \mu\left(\phi_{i,x}\phi_{j,x} + \phi_{i,y}\phi_{j,y}\right) & \underline{0} \\ \underline{0} & \int_{\Omega} \mu\left(\phi_{i,x}\phi_{j,x} + \phi_{i,y}\phi_{j,y}\right) \end{bmatrix} \tag{A-10}$$

$$\underline{\underline{C}} = -\begin{bmatrix} \int_{\Omega} \varphi_j \phi_{i,x} \\ \int_{\Omega} \varphi_j \phi_{i,y} \end{bmatrix} \tag{A-11}$$

$$\underline{f} = \left\{ \int_{\partial\Omega} \phi_i \tilde{\tau}_\alpha \right\} \tag{A-12}$$

where U and V are the velocity components on the x- and y- coordinates, respectively.

The various matrices expressed in (A-9) - (A-11) are spatial integrals of the various interpolation functions and their derivatives. The evaluation of these integrals can be carried out by the use of numerical quadrature procedure.

MORE EFFECTIVE METHOD OF MOISTURE REMOVAL IN THE DRYER

Our computational analyses have shown that eddies form above the dryer rolls in the dryer section. A ventilation device is outlined below which replaces the eddies with a more efficient air stream for moisture removal.

A schematic of the air stream in the dryer unit is presented below in Figure 1. The actual results from the computational analysis are given below in color coded plots of streamlines and velocity vector plots. The colors indicate the magnitude of the dependent variables. The computational results show that recirculating eddies with closed streamlines develop near the dryer roll. This is a potential area for accumulation of moisture which in turn reduces the efficiency of the dryer. With this invention, the eddies are completely removed from the system. This results in less accumulation of moisture and, therefore, a more efficient drying process.

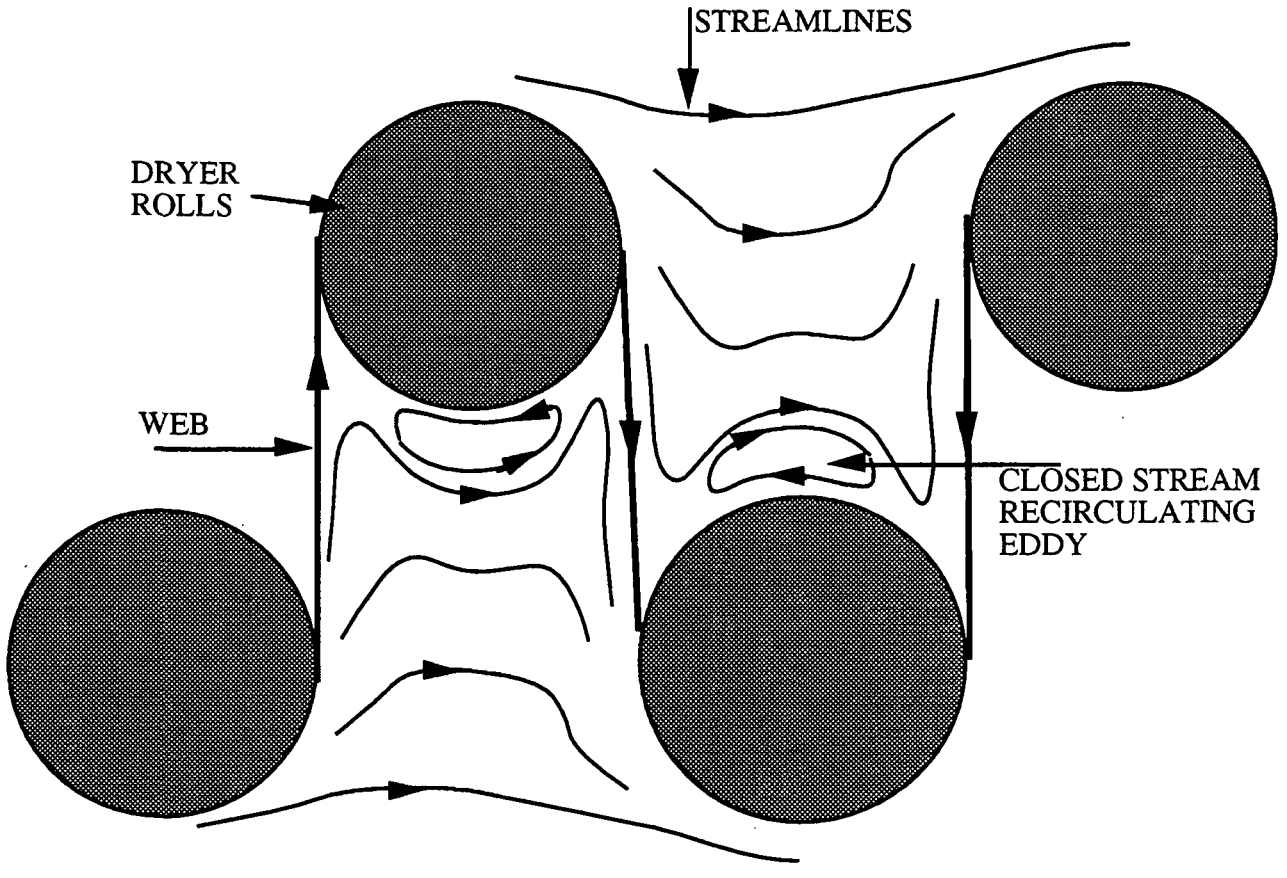

Figure 1. Schematic of the air stream at low speed in the dryer section of a paper machine.

The invention consists of ventilation tubes that are placed at the center of the eddies near the rolls to modify the streamlines and prevent formation of the recirculating eddies, as shown in Figure 2. The ventilation tubes have suction capability at the top portion and air delivery feature at the designated section of the tubes, as shown in Figure 3.

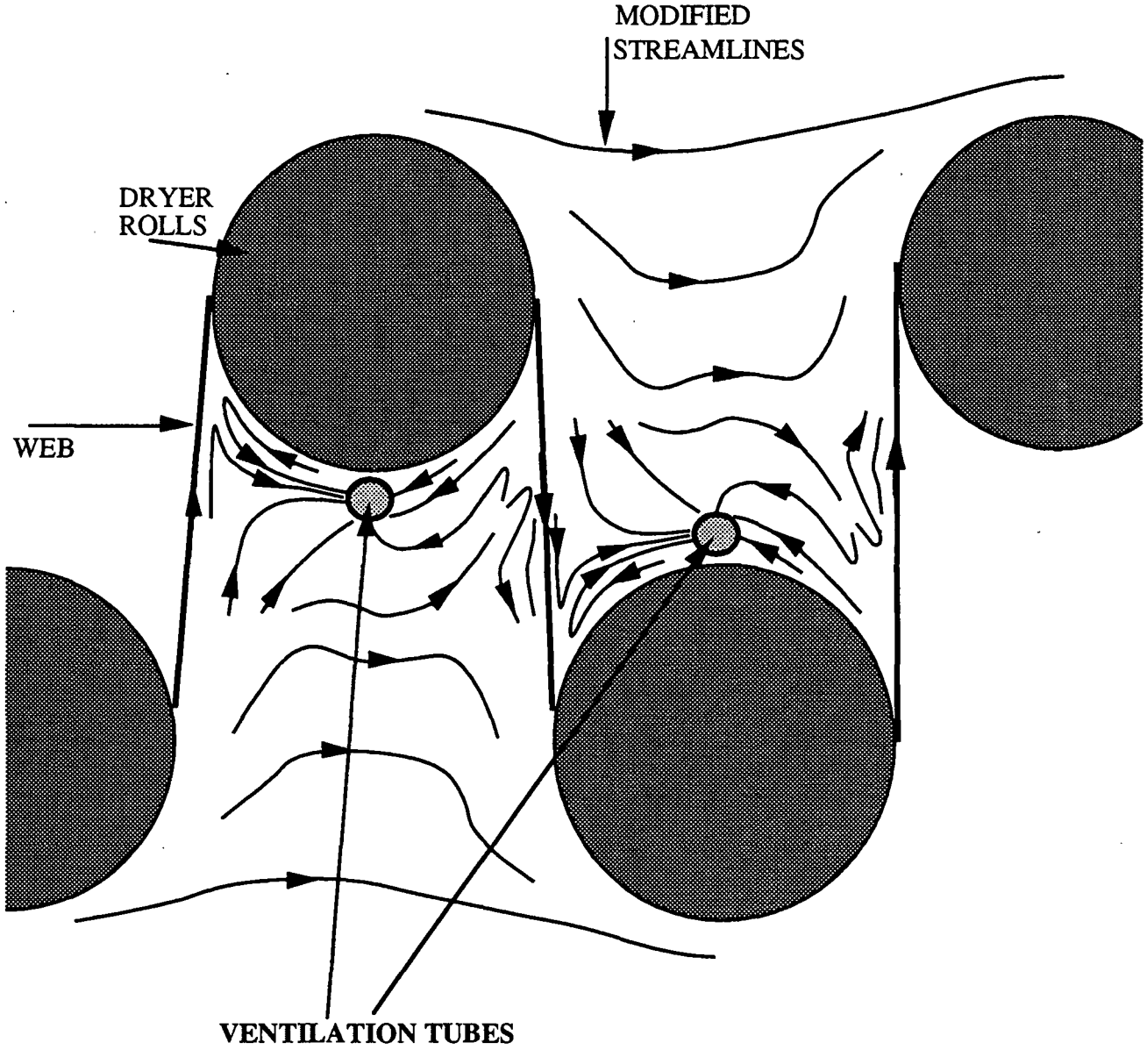

Figure 2. The schematic of the dryer section with ventilation tubes showing the modified streamlines and the destruction of the eddies.

The ventilation tubes can be of different shapes with two primary sections. Depending on the position of the tubes, the top (bottom) portion of the tubes extract (inject) air from (into) the dryer section when the tubes are located above (below) the dryer roll. The drawings in Fig. 3 show three different shapes that can be used effectively to reduce moisture accumulation and to ventilate the system effectively for higher efficiency drying. The shape of the designs depend on the machine speed and the need to streamline the surface of the tube in order to prevent flow separation.

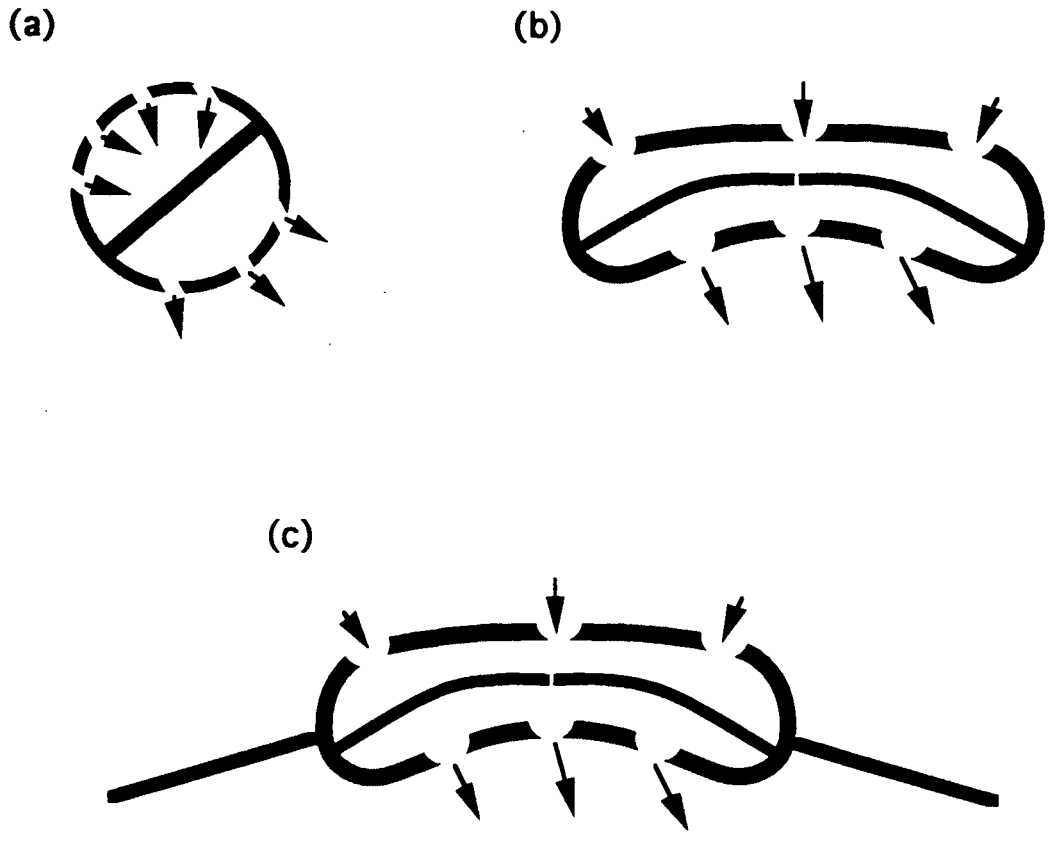

Figure 3. Three different ventilation tubes for removing moisture from the steam rolls in the dryer section. Versions (b) and (c) are aerodynamically designed to prevent further flow separation near the roller for high speed machines. Version (a) is a simple circular tube for low speed machines.

References:

1. Pramila, A. "Sheet Flutter and the Interaction between Sheet and Air", *TAPPI J.*, July 1986, pp. 70 - 74.

2. Pramila, A. "Natural Frequencies of Submerged Axially Moving Band", *Sound and Vibration,* Vol. 113, No. 1, 1987, pp. 198 - 203.

3. Chang, Y., Moretti, P., "Interaction of Fluttering Webs with Surrounding Air ", *TAPPI,* Engineering Conference 1990, pp.175 - 182.

4. Race, E, Wheeldon, J. B., and Fraser-Clark, D., "Air Movement Induced by Felts and Fabrics and its Ventilation Effect on Dryer Pockets",*TAPPI,* Vol. 51, No. 7, July 1968, pp. 51A - 56A.

5. Soininen, M. "The Physics of Paper Machine Sheet Flutter", *International Water Removal Symposium,* 1982, pp. 85 - 86.

6. Sieverding, C. H., Bosche, P. V. "The Use of Coloured Smoke to Visualize Secondary Flows in a Turbine-Blade Cascade", *Journal of Fluid Mechanics*, Vol. 134, 1983 (Revised Form), pp. 85 - 89.

7. Bercovier, M. and M. Engelman, "A Finite Element for the Numerical Solution of Viscous Incompressible Flows", Journal of Computational Physics, Vol. 30, 181-201 (1979).

8. Christoudoulou, K.N. and L.E. Scriven, "The Fluid Mechanics of Slide Coating", Journal of Fluid Mechanics, Vol. 208, 321-354 (1989).

9. Curvelier, C., A. Segal and A.A. v Steenhoven, Finite Element Methods and Navier-Stokes Equations, Reidel, Dordrecht (1986).

10. Gresho, P.M., "Some Interesting Issues in Incompressible Fluid Dynamics, Both in the Continuum and in Numerical Simulation", Advances in Applied Mechanics, Vol. 28, 45-140 (1992).

11. Gresho, P.M., "Incompressible Fluid Dynamics: Some Fundamental Formulation Issues", Annual Review of Fluid Mechanics, Vol. 23, 413-453 (1991).

12. Gresho, P.M. and R.L. Lee, "Don't Suppress the Wiggles - They're Telling You Something!", Computers & Fluids, Vol. 9, 223-253 (1981).

13. Gresho, P.M., R.L. Lee, R.L. Sani and T. Stullich, "On the Time-Dependent FEM Solution of the Incompressible Navier-Stokes Equations in Two- and Three-Dimensions", Recent Advances in Numerical Methods in Fluids, Vol. 1, 27-81, Pineridge Press, Ltd., Swansea, UK (1980).

14. Gunzburg, M.D., Finite Element Methods for Viscous Incompressible Flows. A Guide to Theory, Practice, and Algorithms, Boston, Academic Press (1989).

15. Hinton, E. and J.S. Campbell, "Local and Global Smoothing of Discontinuous Finite Element Functions Using a Least Square Method", International Journal for Numerical Methods in Engineering, Vol. 8, 461-480 (1974).

16. Hood, P. and C. Taylor, "Navier-Stokes Equation using Mixed-Interpolation", in Finite Element Methods in Flow Problems, UAH Press, Huntsville, 57-66 (1974).

17. Hood, P. and C. Taylor, "A Numerical Solution of the Navier-Stokes using FEM Technique", Computers & Fluids, Vol. 1, 73-100, 1973.

18. Hughes, T.J.R., W.K. Liu and A. Brook, "Finite Element Analysis of Incompressible Viscous Flows by the Penalty Function Formulation", Journal of Computational Physics, Vol. 30, 1-60 (1979).

19. Iron, B.M., "A Frontal Solution Program", International Journal for Numerical Methods in Fluids, Vol. 2, 5-32 (1970).

20. Kistler, S.F. and L.E. Scriven, "Coating Flow Theory by Finite Element and Asymptotic Analysis of the Navier-Stokes System", International Journal for Numerical Methods in Fluids, Vol. 4, 207-229 (1984).

21. Lee, R.L., P.M. Gresho and R.L. Sani, "Smoothing Techniques for Certain Primitive Variable Solutions of the Navier-Stokes Equations", International Journal for Numerical Methods in Fluids, Vol. 14, 1785-1804 (1979).

22. Olson, M. and S. Tuann, "Primitive Variables versus Stream Function Finite Element Solutions of the Navier-Stokes Equations", in Finite Element in Fluids, Vol. 3, 73-89, Wiley, Chichester (1978).

23. Patankar, S.V., Numerical Heat Transfer and Fluid Flow, Hemisphere, Washington DC (1980).

24. Pelletier, D.H., A. Fortin and R. Camarero, "Are Solutions of Incompressible Flows Really Incompressible? (Or How Simple Flows Can Cause Headaches!)", International Journal for Numerical Methods in Fluids, Vol. 9, 99-112 (1989).

25. Sackinger, P.A., R.A., Brown and J.J. Derby, "A Finite Element Method for Analysis of Fluid Flow, Heat Transfer, and Free Surfaces in Czochralski Crystal Growth", International Journal for Numerical Methods in Fluids, Vol. 9, 453-492 (1989).

26. Sani, R.L., P.M. Gresho, R.L. Lee and D.F. Griffiths, "The Cause and Cure (?) of the Spurious Pressures Generated by Certain FEM Solutions of the Incompressible Navier-Stokes Equations: Part 1", International Journal for Numerical Methods in Fluids, Vol. 1, 17-43 (1981).

27. Sani, R.L., P.M. Gresho, R.L. Lee, D.F. Griffiths and M. Engelman, "The Cause and Cure (?) of the Spurious Pressures Generated by Certain FEM Solutions of the Incompressible Navier-Stokes Equations: Part 2", International Journal for Numerical Methods in Fluids, Vol. 1, 171-204 (1981).

28. Thomasset, F., Implementation of Finite Element Methods for Navier-Stokes Equations, New York, Springer-Verlag (1981).

ACKNOWLEDGMENT

This member-funded project is a joint effort between the Institute of Paper Science and Technology and the School of Mechanical Engineering at the Georgia Institute of Technology. The windtunnel facilities at the School of Mechanical Engineering have been used for part of these studies. The efforts at Georgia Tech are under the direction of Professor Paul Neitzel. Postdoctoral Associate Shin-Jye Liang is working on the numerical aspects of this project. Maxim Poliashenko is working on the computational stability methods.

Institute of Paper Science and Technology
Atlanta, Georgia

Submitted by:

Cyrus K. Aidun, Ph.D.
Associate Professor of Engineering

Approved by:

David I. Orloff, Ph.D.
Professor of Engineering & Director,
Engineering and Paper Material Division